

Magnetic order in the pseudogap phase of high- T_C superconductors

B. Fauqué¹, Y. Sidis¹, V. Hinkov², S. Pailhès^{1,3}, C.T. Lin², X. Chaud⁴ and P. Bourges^{1,*}

¹ *Laboratoire Léon Brillouin, CEA-CNRS, CEA-Saclay, 91191 Gif sur Yvette, France*

² *MPI für Festkörperforschung, Heisenbergstr. 1, 70569 Stuttgart, Germany*

³ *LNS, ETH Zurich and Paul Scherrer Institute, CH-5232 Villigen PSI, Switzerland*

⁴ *CRETA / CNRS, 25 Avenue des Martyrs, BP 166 38042 Grenoble cedex 9, France.*

One of the leading issues in high- T_C superconductors is the origin of the pseudogap phase in underdoped cuprates. Using polarized elastic neutron diffraction, we identify a novel magnetic order in the $\text{YBa}_2\text{Cu}_3\text{O}_{6+x}$ system. The observed magnetic order preserves translational symmetry as proposed for orbital moments in the circulating current theory of the pseudogap state. To date, it is the first direct evidence of an hidden order parameter characterizing the pseudogap phase in high- T_C cuprates.

In optimally and underdoped regimes, high- T_C copper oxides superconductors exhibit a pseudogap state[1, 2, 3, 4] with anomalous magnetic[5], transport[6], thermodynamic[7] and optical[3] properties below a temperature, T^* , large compared to the superconducting transition temperature, T_c . The origin of the pseudogap is a challenging issue as it might eventually lead to identify the superconducting mechanism[1]. Two major classes of theoretical models attempt to describe the pseudogap state: in a first case, it represents a precursor of the superconducting d -wave gap[8, 9] with preformed pairs below T^* which would acquire phase coherence below T_c [9, 10]. In a second approach, the pseudogap is associated either with an ordered [11, 12, 13, 14, 15, 16] or a disordered phase [1, 17, 18] competing with the SC one. The order parameter, associated with these competing phases may involve charge and spin density waves[14, 15, 16] or charge currents flowing around the CuO_2 square lattice, such as D-charge density wave (DDW) [13] or orbital circulating currents (CC) [11, 12].

Most of these phases break the translation symmetry of the lattice (TSL). Therefore, they may induce charge, nuclear or magnetic superstructures that can be probed by neutron or X-ray diffraction techniques. In contrast, CC phases[11, 12] preserve the TSL as they correspond to 4 or 2 current loops per unit cell (referred as Θ_I and Θ_{II} phases, respectively). These charge currents could be identified by virtue of the pattern of ordered orbital magnetic moments pointing perpendicularly to the CuO_2 planes. These orbital magnetic moments should be detectable by neutron diffraction. Although the TSL is preserved, the magnetic signature of the CC phase does not reduce to ferromagnetism: the loops are staggered within each unit cell corresponding to a zero magnetic propagation wavevector, $\mathbf{Q}=0$, but with no net magnetization. In neutron diffraction, the magnetic intensity superimposes on the nuclear Bragg peak, meaning that these experiments are very delicate as the magnetic intensity $\propto M^2$ (M is the magnetic moment) is expected to be very small as compared to the nuclear Bragg peaks. In order to detect this hidden magnetic response, polarized neutron experiments are then required.

As proposed by C.M. Varma[11, 12], there are two possible CC phases preserving TSL. The first (the phase Θ_I) has not been detected by polarized elastic neutron scattering experiments [19, 20]. Although it is controversial, a recent ARPES measurement observed a dichroic signal in the $\text{Bi}_2\text{Sr}_2\text{CaCu}_2\text{O}_{8+\delta}$ system consistent with the phase Θ_{II} [21]. Here, we have performed polarized elastic neutron scattering experiments to test the magnetic moments of this second CC state, phase Θ_{II} , which actually had never been attempted before. We successfully report the first signature of a novel magnetic order in the pseudogap state of $\text{YBa}_2\text{Cu}_3\text{O}_{6+x}$ (YBCO). The pattern of the observed magnetic scattering corresponds to the one expected in the circulating current theory of the pseudogap state with two current loops per CuO_2 unit-cell, phase Θ_{II} [11, 12]. Alternatively, a decoration of the unit cell with staggered moments on the oxygen sites could also account for the measurements.

All the polarized neutron diffraction measurements were collected on the 4F1 triple-axis spectrometer at the Laboratoire Léon Brillouin (LLB), Saclay (France). Our polarized neutron diffraction setup is similar to that originally described in [22] with a polarized incident neutron with at $E_i = 14.7$ meV obtained with a polarizing supermirror (bender) and with an Heusler analyzer (see also ref. [19, 23] in the context of high- T_C cuprates). The direction of the neutron spin polarization, \mathbf{P} , at the sample position is selected by a small guide field \mathbf{H} of the order of 10 G[24]. Using that configuration, we monitor for each measured point the neutron scattering intensity in the spin-flip (SF) channel, where the magnetic intensity $\propto M^2$ is expected, and in the non-spin-flip (NSF) channel which measures the nuclear scattering. To have similar counting statistics on both SF and NSF, we count the SF channel systematically 20 times longer than the NSF. We define the normalized spin-flip intensity as $I_{norm} = I_{SF}/I_{NSF}$ (inverse of the flipping ratio (FR)). With that setup, a typical flipping ratio, ranging between 40 and 60, is obtained. However, even with that high FR, the SF intensity is massively coming from the NSF nuclear Bragg peak through unavoidable polarization leakage (corresponding to about ~ 90 -95%

label	x	$T_{c,onset}$ (K)	T_{mag} (K)	References
A	$O_{6.5}(t)$	ud 54	300 ± 10	[23]
B	$O_{6.6}(t)$	ud 61	250 ± 20	[30]
C	$O_{6.6}(d)$	ud 64	220 ± 20	[29]
D	$O_{6.75}(t)$	ud 78	170 ± 30	-
E	$Ca(15\%) - O_{7-\delta}(t)$	od 75	$\simeq 0$	-

TABLE I: List of samples utilized in the polarized elastic neutron experiments. The experiments were performed in the $(Y,Ca)Ba_2Cu_3O_{6+x}$ family for 5 samples from the underdoped (ud) to overdoped (od) part of the cuprates phase diagram. (t) and (d) stands for twinned and detwinned samples, respectively. References are given where the samples have been described in previous neutron scattering studies. In contrast to the other samples, an in-plane magnetic ordering occurred at $\mathbf{Q}=(1/2,1/2)$ in sample A with $M \sim 0.05\mu_B$ at 60 K[23].

of the SF intensity). As a very stable and homogeneous neutron polarization is essential through the data acquisition, all the data have been obtained in a continuous run versus temperature. We prove that method to be efficient enough to see weak magnetic moments ($\sim 0.05\mu_B$) on top of nuclear Bragg peaks, see e.g. the first determination of the A-type antiferromagnetism in Na cobaltate systems[25].

We quote the scattering wave vector as $\mathbf{Q}=(H,K,L)$ in units of the reciprocal lattice vectors, $a^* \sim b^* = 1.63 \text{ \AA}^{-1}$ and $c^* = 0.53 \text{ \AA}^{-1}$. Most of the data have been obtained in a scattering plane where all Bragg peaks like $\mathbf{Q}=(0,K,L)$ were accessible (in twinned samples, this is indistinguishable from Bragg peaks with $\mathbf{Q}=(H,0,L)$). In order to evidence small magnetic moments, measurements have been performed on the weakest nuclear Bragg peaks having the proper symmetry for the CC phase[26] (the Bragg peak $\mathbf{Q}=(0,1,1)$ offers the best compromise).

We have studied 5 different samples (see Table I): 4 samples in the underdoped regime and one in the overdoped regime. In Fig. 1.a, we report the raw neutron intensity measured at $\mathbf{Q}=(0,1,1)$ for the spin flip (SF) channel and for the non-spin-flip (NSF) channel for an underdoped sample $YBa_2Cu_3O_{6.6}(d)$ (sample C). The measurement has been done with a neutron polarization $\mathbf{P} // \mathbf{Q}$ (see Fig. 1.b) where the magnetic scattering is entirely spin-flip[19, 22, 23, 24]. Between room temperature and a temperature $T_{mag} \simeq 220K$, the NSF and SF intensities display the same evolution within error bars. Then, for $T < T_{mag}$, the NSF is essentially flat whereas the SF intensity increases noticeably at low temperature. This behaviour signals the presence of a spontaneous magnetic order below T_{mag} on top of the nuclear Bragg peaks. In Fig. 1.c, we show the normalized magnetic intensity as a function of the temperature for the 4 underdoped samples and the overdoped sample. For the 4 underdoped samples, the magnetic intensity increases at low temperature

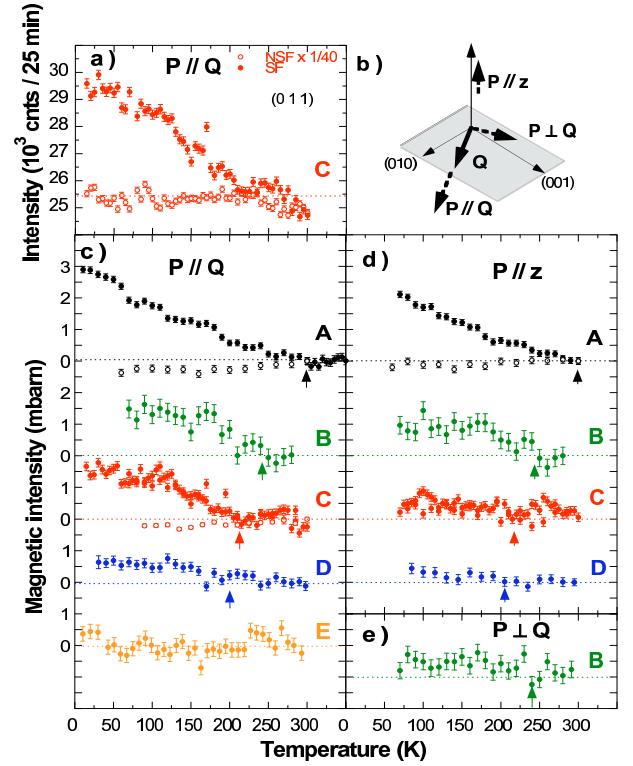


FIG. 1: (color online) (a): Temperature dependencies of the raw SF and NSF neutron intensity measured at $\mathbf{Q}=(0,1,1)$ in sample C. (b) Sketch of the scattering plane showing the three polarization directions discussed here, $\mathbf{P} // \mathbf{z}$ corresponds to the direction perpendicular to the scattering plane (here a^*). (c) Temperature dependencies of the normalized magnetic intensity, I_{mag} , measured at $\mathbf{Q}=(0,1,1)$ for $\mathbf{P} // \mathbf{Q}$ for the 4 underdoped samples (A,B,C,D) and the overdoped sample E (full points). I_{mag} is defined as $I_{mag}(T) = \alpha I_{NSF}(300K) \left[\frac{I_{SF}}{I_{NSF}}(T) - \frac{I_{SF}}{I_{NSF}}(T \sim 300K) \right]$ where (i) I_{mag} is arbitrarily set to zero in the high temperature range (\sim room temperature), (ii) $\alpha = 7/I_{004}^{meas}(300K)$ calibrates the magnetic cross-sections in mbarns using the nuclear Bragg cross-section at $\mathbf{Q} = (0, 0, 4)$, $I_{004}^{calc} = 7$ barns. The normalized magnetic intensity for the Bragg peak, $\mathbf{Q} = (0, 0, 2)$, is also shown for samples A and C (open points). (d) Temperature dependencies of the normalized magnetic intensity measured at $\mathbf{Q}=(0,1,1)$ (full points) (as well as $\mathbf{Q}=(0,0,2)$, open points) for $\mathbf{P} // \mathbf{z}$. (e) Temperature dependencies of the normalized magnetic intensity, I_{mag} , measured at $\mathbf{Q}=(0,1,1)$ for sample B for $\mathbf{P} \perp \mathbf{Q}$.

below a certain temperature T_{mag} whereas no magnetic signal is observed in the Ca-YBCO overdoped sample (sample E).

We perform further measurements where the neutron polarization is along the complementary directions, as shown in Fig. 1.b, either the vertical direction $\mathbf{P} // \mathbf{z}$, or $\mathbf{P} \perp \mathbf{Q}$ but still within the horizontal scattering plane. The observance of the polarization selection rule for a

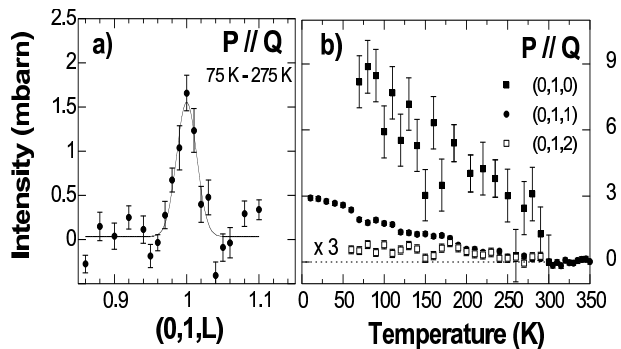


FIG. 2: a) L-scan magnetic intensity across $Q=(0,1,L)$ in sample A: it has been obtained using the following relation of measured quantities $[I(SF, 75K) - I(SF, 275K)] \frac{I(NSF, 75K)}{I(NSF, 275K)}$ calibrated by α (see caption Fig. 1). b) Temperature dependencies of the magnetic intensity, I_{mag} , for various Bragg peaks $L=0,1,2$ in sample A.

magnetic signal, $I_{\mathbf{P} // \mathbf{Q}} = I_{\mathbf{P} // \mathbf{z}} + I_{\mathbf{P} \perp \mathbf{Q}}$, in the three polarizations, as shown in Fig. 1.c, 1.d and 1.e for sample B, unambiguously demonstrates the magnetic origin of the low temperature signal. More precisely, in the $\mathbf{P} // \mathbf{z}$, configuration, only magnetic moments within the horizontal scattering plane but still perpendicular to \mathbf{Q} are observed in SF channel [19, 22, 23, 24]. For $\mathbf{Q} = (0, 1, 1)$, this means that we mostly probe the magnetic moments parallel to the c^* axis. In the 4 underdoped samples, we observe a similar onset of the magnetic order below T_{mag} for $\mathbf{P} // \mathbf{z}$ (Fig. 1.d). This demonstrates that the deduced magnetic moment has a well-defined component perpendicular to the CuO_2 plane. However, a closer comparison with both polarizations reveals that their intensities do not simply match. This underlines that the magnetic moment also exhibits an in-plane component (within the CuO_2 plane) as the cross-section in Fig. 1.c is larger than the one in Fig. 1.d. Combining all measured polarizations in the different samples, one can then estimate a mean angle between the direction of the moments with the c^* axis to be $\phi = 45^\circ \pm 20^\circ$ valid for all samples.

As shown in Fig. 1.c, the typical cross-section of the magnetic order is $\sim 1-2$ mbarns, *i.e.* $\sim 10^{-4}$ of the strongest Bragg peaks. This explains why such a magnetic order was not reported before with unpolarized neutron diffraction. Due to these experimental limitations, we do not perform a detailed and quantitative determination of magnetic structure for which further work is needed. However, some qualitative aspects can be briefly discussed. First, we perform a scan along the L-direction in the SF channel across the Bragg peak (Fig. 2.a) where the difference in temperature between $T=75$ K and 275 K has been taken to remove the effect of the polarization leakage. The observed magnetic peak is resolution limited, showing that the magnetic order is character-

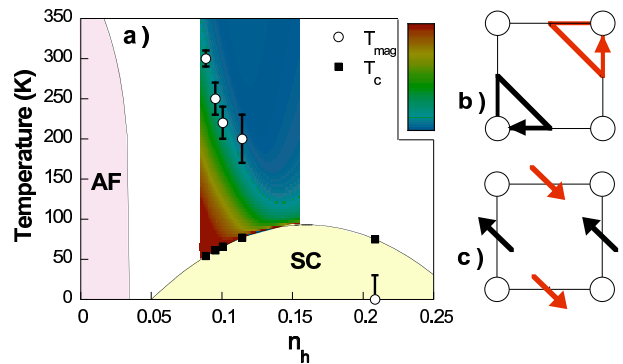


FIG. 3: (color online) a) Cuprate superconductors phase diagram as a function of hole doping, n_h , deduced from the SC temperature using the empirical relation $T_C/T_C^{max} = 1 - 82.6(n_h - 0.16)^2$ [31]. The white points show T_{mag} (see table I). The color map shows the quantity $\delta R(T) = 1 - [\rho_{ab}(T) - \rho_{ab}(0)]/(\alpha T)$ deduced from the resistivity measurements in YBCO[6]: the change of colors indicates the departure from the T-linear behaviour, $\delta R(T) = 0$ represented in blue, at high temperature. $\delta R(T) \neq 0$ defines the pseudogap state. b) Circulating current phase, Θ_{II} , in the CuO_2 plane proposed to explain the pseudogap phase in high- T_C superconducting cuprates[11, 12]. c) A spin model preserving TSL.

ized by long range 3D correlations at $T=75$ K. Second, by looking at other Bragg peaks along c^* (Fig. 2.b), we found that the magnetic intensity is not uniformly distributed versus L , meaning that i) the magnetic intensity does not arise from the Cu-O chains, and ii) the moments arrangement within a bilayer appears to be mainly parallel. This directly arises from the hierarchy of the observed magnetic intensities (intensity at $L=0$ is larger than at $L=2$, Fig. 2.b). Finally, using the observed magnetic cross-section (Fig. 1.c) and a weakly momentum dependent form factor, one can deduce a typical magnitude of ordered magnetic moment of $M \simeq 0.05$ to $0.1\mu_B$ with the moment decreasing with increasing doping in the 4 samples.

Therefore, we observe an unusual magnetic order in a temperature and doping range that cover the range where the pseudogap state is observed in YBCO. Our data do not contradict previous unsuccessful polarized neutron reports[19] as the Bragg spots where the effect is observed are along a direction at 45° from the one previously studied[26]. The deduced T_{mag} , defined as the change of slope in the normalized intensity I_{mag} , decreases with increasing doping (see table I). It matches the pseudogap temperature, T^* , of the resistivity data in YBCO[6] as shown on Fig. 3. The occurrence of a magnetic order in this temperature and doping ranges points towards a magnetic signature of a hidden order parameter associated with the pseudogap state. As all

anomalous physical properties evidencing the pseudogap, the temperature dependence of the magnetic order does not exhibit a marked change at T_{mag} . Being on top of nuclear Bragg peaks, that magnetic order does not break TSL, indicating a zero magnetic propagation wavevector, $\mathbf{Q} = 0$. As shown in Fig. 1.c, no magnetic intensity occurs below T_{mag} at the Bragg peak $\mathbf{Q} = (0, 0, 2)$, ruling out a ferromagnetic order. The absence of breaking of TSL points towards a magnetic pattern of antiparallel magnetic moments within each unit cell. Among the proposed order parameters, only one gives magnetic scattering at $\mathbf{Q} = (10L)[\equiv (01L)]$: it is the orbital moments arising from the circulating current phase with 2 current loops per CuO_2 unit cell, Θ_{II} (Fig. 3.b) [11, 12]. Another possibility could be a model with colinear spin moments located at the oxygen site ferromagnetic along both directions of the square lattice but antiparallel each other as sketched on Fig. 3.c. Any other model characterized by a decoration of the CuO_2 plaquette would also give rise to a magnetic contribution at the proper Bragg spots.

From our present measurements, one cannot distinguish between these two models. Only a detailed study of magnetic form factors would allow to differentiate the scattering from spin and orbital moments. However, some arguments can be given from the observed moments direction, which is not within the CuO_2 plane neither perpendicular to it. Clearly, an in-plane magnetic component is not expected within the orbital moments picture of currents flowing within perfectly flat CuO_2 planes. However, due to the dimpling of CuO_2 planes in YBCO, the moments can be tilted by about 11° from the c axis as the effective moments at the centers of the O-Cu-O plaquettes are perpendicular to these plaquettes. Within an orbital moment picture, spin degree of freedom might also play a role in producing in-plane magnetic moments, for instance, by spin-orbit scattering[27] or in relation to chiral spin states associated with flux phases [28]. Alternatively, if considering spin models, one would rather expect moments lying within the CuO_2 plaquette as it is the case for copper spins in undoped cuprates. A reason should be found to explain why the moments exhibit an out-of-plane component. Whatever the origin of the observed order, its pattern challenges the single band Hubbard picture commonly used to describe high- T_C cuprates. At very least, oxygen orbitals need to be included to determine the minimal effective Hamiltonian for the cuprates.

In conclusion, we report a first signature of an unusual magnetic order in several $\text{YBa}_2\text{Cu}_3\text{O}_{6+x}$ samples matching the pseudogap behaviour in underdoped cuprates (Fig. 3). Such an observation points towards the existence of an hidden order parameter for the pseudogap phase in high- T_C superconductors. Importantly, our experiment reveals that a 3D long range order does not break the translational symmetry of the lattice and im-

plies a decoration of the unit cell with staggered spin or orbital moments. The symmetry of the observed order corresponds to the one expected in orbital moments emanating from a circulating current state [11, 12].

We are very grateful to C.M. Varma for invaluable encouragement, critics and ideas on these experiments. We also thank B. Keimer, J.-M. Mignot, P. Monceau, L. Pintschovius, and L.-P. Regnault for their support.

*To whom correspondence should be addressed; E-mail: bourges@llb.saclay.cea.fr

-
- [1] M.R. Norman, D.P. Pines, & C. Kallin, preprint cond-mat/0507031.
 - [2] M.R. Norman & C. Pépin, *Rep. Prog. Phys.* **66**, 1547 (2003).
 - [3] T. Timusk, & B. Statt, *Rep. Prog. Phys.* **62**, 61 (1999).
 - [4] J.L. Tallon & J.W. Loram, *Physica C* **349**, 53 (2001).
 - [5] H. Alloul *et al.* *Phys. Rev. Lett.* **63**, 1700 (1989).
 - [6] T. Ito *et al.* *Phys. Rev. Lett.* **70**, 3995 (1993).
 - [7] J.W. Loram *et al.* *Physica C*, **235-240** 134 (1994).
 - [8] P.A. Lee, *Physica C* **317-318**, 194-204, (1999).
 - [9] V.J. Emery & S.A. Kivelson, *Nature* **374**, 434 (1995).
 - [10] J. Orenstein, & A.J. Millis, *Science* **288**, 468 (2000).
 - [11] C.M. Varma, *Phys. Rev. B*, **55**, 14554 (1997); *Phys. Rev. Lett.* **83**, 3538 (1999); preprint, cond-mat/0507214.
 - [12] M.E. Simon & C.M. Varma, *Phys. Rev. Lett.* **89**, 247003 (2002).
 - [13] S. Chakravarty *et al.* *Phys. Rev. B* **63**, 094503 (2001).
 - [14] C. Castellani *et al.* *Phys. Rev. Lett.* **75**, 4650 (1995).
 - [15] H.C. Chen, *et al.* *Phys. Rev. Lett.* **93**, 187002 (2004).
 - [16] D. Poilblanc, cond-mat/0503249.
 - [17] J. Zaanen, *et al.* *Phil. Mag. B*, **81**, 1485 (2001).
 - [18] F. Onufrieva, P. Pfeuty, *Phys. Rev. Lett.*, **82**, 3136 (1999).
 - [19] S.H. Lee *et al.* *Phys. Rev. B* **60**, 10405 (1999).
 - [20] Ph. Bourges, L.P. Regnault, J.Y. Henry, & C. Marin, Unpublished data (1998).
 - [21] A. Kaminski, *et al.*, *Nature* **416**, 610 (2002); S. Borisenko, *et al.*, *Nature* **431**, (2 September 2004); A. Kaminski, *et al.*, *ibid.*
 - [22] R.M. Moon *et al.* *Phys. Rev.* 181, 920 (1969).
 - [23] Y. Sidis, *et al.* *Phys. Rev. Lett.* **86**, 4100 (2001).
 - [24] Magnetic neutron diffraction always measures magnetic components perpendicular to the scattering wavevector. In a polarized experiment, only the magnetic components perpendicular to the neutron polarization direction contributes to the spin-flip channel[22].
 - [25] S.P. Bayrakci *et al.* *Phys. Rev. Lett.* **94**, 157205 (2005).
 - [26] Bragg magnetic peaks characteristic of the two CC states proposed[12] differ by 45° : main Bragg peaks like $\mathbf{Q} = (11L)$ are expected for the state Θ_I and like $\mathbf{Q} = (10L)[\equiv (01L)]$ for the state Θ_{II} . In both cases, no magnetic contribution occurs on Bragg peaks like $\mathbf{Q} = (00L)$.
 - [27] C. Wu, Y. Zaanen & S.C. Zhang, cond-mat/0505544.
 - [28] X.G. Wen *et al.* *Phys. Rev. B*, **39**, 11413 (1989).
 - [29] V. Hinkov *et al.*, *Nature* **430**, 650 (2004).
 - [30] L. Pintschovius *et al.*, *Phys. Rev. Lett.* **89**, 037001 (2002).
 - [31] J.L Tallon *et al.*, *Phys. Rev B*, **51**, R12911 (1995).